

# Silibinin inhibits epithelial-mesenchymal transition of renal cell carcinoma through autophagy-dependent Wnt/ $\beta$ -catenin signaling

YIZENG FAN\*, TAO HOU\*, WEICHAO DAN, TIANJIE LIU, JIAXIN LUAN, BO LIU, LEI LI and JIN ZENG

Department of Urology, The First Affiliated Hospital of Xi'an Jiaotong University, Xi'an, Shaanxi 710061, P.R. China

Received October 9, 2019; Accepted January 22, 2020

DOI: 10.3892/ijmm.2020.4521

**Abstract.** Silibinin is a flavonoid extracted from milk thistle seeds which has been widely used as a hepatoprotective and antioxidant agent. Recently, accumulating evidence has demonstrated the anti-cancer effects of silibinin in various cancer models. It was previously reported that silibinin induced apoptosis and decreased metastasis by activating autophagy in renal cell carcinoma (RCC). However, the underlying molecular mechanisms by which silibinin regulates autophagy remain largely unknown. The aim of the present study was to investigate the effects of silibinin on RCC metastasis *in vitro* and *in vivo*, with a focus on autophagy-dependent Wnt/ $\beta$ -catenin signaling. Human RCC 786-O and ACHN cell lines were used as the model system *in vitro* and RCC xenografts of nude mice were used for *in vivo* studies. Silibinin inhibited metastasis and epithelial-mesenchymal transition (EMT) of RCC *in vitro* and *in vivo*, by regulating the Wnt/ $\beta$ -catenin signaling pathway. Furthermore, silibinin inhibited the Wnt/ $\beta$ -catenin signaling pathway in an autophagy-dependent manner. Autophagic degradation of  $\beta$ -catenin induced by silibinin was associated with the anti-metastatic effects of silibinin against RCC. These findings identify a novel mechanism by which silibinin inhibits EMT and metastasis of RCC, highlighting a potential novel strategy for treating metastatic RCC.

## Introduction

Renal cell carcinoma (RCC) is a common disease of the urinary tract which accounts for 2-3% of all adult malignant tumors (1). Clear cell RCC is the most common type of RCC

and is present in 30% of patients with RCC with evidence of metastasis at the initial diagnosis (2). In China, the morbidity of patients with kidney cancer has increased in recent years, which clearly poses a serious public health problem. Surgery remains the most effective option for localized treatment as RCC is often insensitive to traditional chemotherapy and radiotherapy (3). Targeted therapy has been widely used in patients with advanced metastatic RCC; however, a significant number of patients exhibited limited benefits. Therefore, a novel and more efficient therapeutic regimen is required.

Silibinin, a flavonoid extracted from milk thistle seeds, is widely used as a hepatoprotective and antioxidant agent in Asia and Europe (4). Previously, accumulating evidence from the authors' and other research laboratories has demonstrated the anti-cancer effects of silibinin in various models of cancer (4-16). The authors' laboratory has focused on the mechanisms underlying silibinin mediated suppression of metastasis in different types of urological cancer, including RCC, prostate cancer and bladder cancer. In RCC, the authors' previously demonstrated that silibinin decreased invasion and migration of RCC 786-O cells *in vitro* and this was associated with downregulation of matrix metalloproteinase (MMP)-2 and 9, and urokinase plasminogen activator, and inhibition of the mitogen-activated protein kinase pathway. Additionally, silibinin decreased migration and invasion of RCC cells by suppressing epidermal growth factor receptor/MMP-9 signaling (17) and decreased the metastatic capacity of RCC by activating autophagy through adenosine 5'-monophosphate-activated protein kinase (AMPK)/mammalian target of rapamycin (mTOR) pathway (18). However, the molecular mechanisms underlying regulation of autophagy are largely unknown.

In the present study, the anti-metastatic effects of silibinin on RCC were determined, with a focus on autophagy-dependent Wnt/ $\beta$ -catenin signaling. The results suggest that silibinin exerted its anti-metastatic effects on RCC through inhibition of the epithelial-mesenchymal transition (EMT). Mechanistically, autophagy-dependent Wnt/ $\beta$ -catenin signaling is involved in the inhibition of metastasis and EMT by silibinin in RCC.

## Materials and methods

**Cell culture.** Human RCC cell lines, 786-O and ACHN were obtained from the American Type Culture Collection, and maintained in RPMI-1640 medium (Gibco; Thermo Fisher Scientific, Inc.) with 10% fetal bovine serum (FBS; Gibco;

---

*Correspondence to:* Professor Jin Zeng or Professor Lei Li, Department of Urology, The First Affiliated Hospital of Xi'an Jiaotong University, 277 Yanta West Road, Xi'an, Shaanxi 710061, P.R. China  
E-mail: zengjin1984@gmail.com  
E-mail: lilydr@163.com

\*Contributed equally

**Key words:** silibinin, metastasis, epithelial-mesenchymal transition, autophagy, Wnt/ $\beta$ -catenin signaling

Thermo Fisher Scientific, Inc.) at 37°C with 5% CO<sub>2</sub> in a humidified atmosphere. The culture medium was supplemented with 100 U/ml penicillin and 0.1 mg/ml streptomycin (Gibco; Thermo Fisher Scientific, Inc.).

**Reagents and antibodies.** Silibinin was purchased from Sigma-Aldrich; Merck KGaA and dissolved to a final concentration of 50 mM in DMSO. Hydroxychloroquine sulfate (cat. no. H0915), 3-Methyladenine (3-MA; cat. no. M9281) and lithium chloride (LiCl; cat. no. L9650) were purchased from Sigma-Aldrich; Merck KGaA. Recombinant human transforming growth factor- $\beta$ 1 (TGF- $\beta$ 1; cat. no. 240-B) was purchased from R&D Systems, Inc., and used at a concentration of 5 ng/ml. Rabbit primary antibodies against vimentin (cat. no. 5471; 1:2,000), Wnt3a (cat. no. 2721; 1:500), phosphorylated  $\beta$ -catenin (Ser33/37; cat. no. 2009; 1:500), total  $\beta$ -catenin (cat. no. 8480; 1:1,000), phosphorylated glycogen synthase kinase (GSK)3 $\beta$  (Ser9; cat. no. 5558; 1:1,000), total GSK3 $\beta$  (cat. no. 12456; 1:1,000), autophagy-associated gene 5 (ATG5; cat. no. 9980; 1:1,000) and  $\beta$ -actin (cat. no. 4970; 1:5,000) were all purchased from Cell Signaling Technology, Inc. Antibodies against LC3B (cat. no. ab48394; 1:1,000), epithelial (E)-cadherin (cat. no. ab15148; 1:2,000), neural (N)-cadherin (cat. no. ab76057; 1:1,000), Histone H3 (cat. no. ab176842; 1:1,000) and GAPDH (cat. no. ab181602; 1:5,000) were purchased from Abcam.

**MTT assay.** RCC cells were plated into 96-well culture plates and treated with various concentrations of silibinin for 24 h. The supernatant of each well was replaced with fresh medium containing 10% MTT (5 mg/ml) and incubated for a further 4 h. Subsequently, the medium was removed and 150  $\mu$ l DMSO was added to each well. A 96-well microplate reader (Bio-Rad Laboratories, Inc.) was used to detect the absorbance at 570 nm.

**Wound healing assay.** RCC cells were seeded at a density of 20.0x10<sup>4</sup> cells/well into 6-well plates and cultured. Wounds were created by scratching with a 200- $\mu$ l pipette tip when the cells had grown to 90-100% confluence. The fragments of RCC cells were washed with PBS and incubated in serum-free media with or without silibinin. Wound closure was observed at 0, 12, 24 and 36 h using an inverted microscope (magnification, x40). The average area of the wound was calculated using ImageJ v1.47 software (National Institute of Health). The wound closure (% of control) was calculated using the following formula: Wound closure (% of control)=(gap closure of silibinin treatment group/gap closure of control group) x100.

**Transwell migration and invasion assays.** For migration assays, 0.2 ml FBS-free RPMI-1640 medium suspension with 2x10<sup>4</sup> RCC cells were seeded into the upper chamber in a 24-well plate and 0.8 ml supplemented RPMI-1640 medium was added to the lower chamber. After incubating for 24 h, the chamber was washed with PBS and fixed at room temperature with 4% formalin for 15 min. Subsequently, the chamber was stained at room temperature with crystal violet (0.1%, dissolved in the ethanol) for 25 min. For invasion assays, a 50  $\mu$ l mixture of FBS-free RPMI-1640/Matrigel at 10:1 ratio (Matrigel was obtained Sigma-Aldrich; Merck KGaA) was plated onto the

upper chamber. RCC cells were incubated for 36 h and the rest protocol was performed as described for the migration assay. An inverted microscope was used to count the number of cells which had migrated or invaded in 5 randomly selected fields (magnification, x100). The migration or invasion index (%) was calculated using the following formula: Migration/invasion index (%)=(average transmembrane number of silibinin treatment group/average transmembrane number of control group) x100.

**Western blot analysis.** Cells were washed with ice-cold PBS and lysed with radioimmunoprecipitation assay buffer (50 mM Tris, 150 mM NaCl, 0.1% SDS, 1% NP40 and 0.5% sodium deoxycholate; pH 7.4) containing proteinase inhibitors (cat. no. 04693132001; Sigma-Aldrich; Merck KGaA) and phosphatase inhibitors (cat. no. 04906837001; Sigma-Aldrich; Merck KGaA). The lysates were centrifuged at 15,000 x g at 4°C for 15 min and 5  $\mu$ g cell supernatant lysate was used to detect the concentration of proteins using a Bradford assay. A total of 30  $\mu$ g proteins was loaded onto a 10 or 15% SDS gel and resolved by SDS-PAGE. Proteins were transferred onto PVDF membranes. The membranes were blocked with 5% BSA for 1 h at room temperature and subsequently incubated with primary antibodies [vimentin (cat. no. 5741; dilution, 1:2,000; Cell Signaling Technology, Inc.), Wnt3a (cat. no. 2721; dilution, 1:500; Cell Signaling Technology, Inc.), phosphorylated  $\beta$ -catenin (Ser33/37; cat. no. 2009; dilution, 1:500; Cell Signaling Technology, Inc.), total  $\beta$ -catenin (cat. no. 8480; dilution, 1:1,000; Cell Signaling Technology, Inc.), phosphorylated glycogen synthase kinase (GSK)3 $\beta$  (Ser9; cat. no. 5558; dilution, 1:1,000; Cell Signaling Technology, Inc.), total GSK3 $\beta$  (cat. no. 12456; dilution, 1:1,000; Cell Signaling Technology, Inc.), autophagy-associated gene 5 (ATG5; cat. no. 9980; dilution, 1:1,000; Cell Signaling Technology, Inc.) and  $\beta$ -actin (cat. no. 4970; dilution, 1:5,000; Cell Signaling Technology, Inc.), LC3B (cat. no. ab48394; dilution, 1:1,000; Abcam), epithelial (E)-cadherin (cat. no. ab15148; dilution, 1:2,000; Abcam), neural (N)-cadherin (cat. no. ab76057; dilution, 1:1,000; Abcam), Histone H3 (cat. no. ab176842; dilution, 1:1,000; Abcam) and GAPDH (cat. no. ab181602; dilution, 1:5,000; Abcam)] overnight at 4°C. After incubation with the primary antibodies the membranes were washed with TBS with 0.1% Tween-20 and incubated with the anti-rabbit IgG peroxidase antibody produced in goat (cat. no. A9169; dilution, 1:5,000; Sigma-Aldrich; Merck KGaA) for 1 h at room temperature. Signals were visualized using Clarity Max Western ECL substrate (cat. no. 1705062; Bio-Rad Laboratories, Inc.), followed by exposure to X-ray films.  $\beta$ -actin was used as the loading control.

**Co-immunoprecipitation.** Cells were lysed with immunoprecipitation (IP) buffer (50 mM Tris HCl, 150 mM NaCl, 1 mM ethylenediaminetetraacetic acid, 1% Triton X-100) with protease inhibitors and phosphatase inhibitors (5). After incubation with an LC3B antibody (20  $\mu$ g per 500  $\mu$ g of protein; cat. no. ab48394; Abcam) for 12 h at 4°C, Protein G Dynabeads were applied to bind with the LC3B antibody for 3 h at 4°C. Subsequently, cell lysates were washed twice with IP buffer and boiled at 95°C for 5 min. Finally, proteins were subjected to western blotting.

**Small interfering (si)RNA and plasmid transfections.** siRNAs targeting specific genes and non-specific control (NC) were purchased from Shanghai GenePharma Co., Ltd. siRNA transfections were used to silence the expression of  $\beta$ -catenin and ATG5 in RCC cells. The corresponding negative control (si-NC) 5'-UUCUCCGAACGUGUCACGUTT-3' was designed and synthesized by Guangzhou RiboBio Co., Ltd. The sequences of the siRNAs against ATG5 were: ATG5 siRNA (si-ATG5) sequence 1, 5'-GAAGTTTGTCTTCTGCTA-3' and sequence 2, 5'-CAAUCCCAUCCAGAGUUGCTT-3'. The sequences of the siRNAs against  $\beta$ -catenin were: siRNA  $\beta$ -catenin (si- $\beta$ -catenin) sequence 1, 5'-CCUUCACUC AAGAACAAGUTT-3' and sequence 2, 5'-GCUCAUCAU ACUGGCUAGUTT-3'.  $\beta$ -catenin cDNA was cloned into a pcDNA3.1 vector. For transfection, a 1:1 mixture of the siRNAs or plasmid with Lipofectamine<sup>®</sup> 2000 (Invitrogen; Thermo Fisher Scientific, Inc.) was added to the serum free medium according to the manufacturer's protocol. At 48 h after transfection, reverse transcription-quantitative PCR and western blot analyses were used to determine transfection efficiency.

**Immunofluorescence staining.** 786-O and ACHN cells were plated on glass coverslips and treated with silibinin for 24 h. Cells were fixed at room temperature with 4% formaldehyde for 20 min and washed with PBS three times. A 0.5% Triton X-100 solution was used to permeate the cells for 20 min, after which the cells were washed with PBS three times. The cells were incubated with primary antibodies against  $\beta$ -catenin (cat. no. 8480; dilution, 1:200; Cell Signaling Technology, Inc.) overnight at 4°C and subsequently washed with PBS three times. Cells were subsequently incubated with goat anti-rabbit IgG H&L fluorescein isothiocyanate (FITC) (cat. no. ab6717; cat. no. 1:200; Abcam) for 1 h at room temperature. RCC cells were counterstained with DAPI (1  $\mu$ g/ml) for 5 min.  $\beta$ -catenin expression was detected on a confocal laser scanning microscope.

**Preparation of cytoplasmic and nuclear extracts.** 786-O and ACHN cells were treated with the indicated doses of silibinin for 24 h. Cytoplasmic and nuclear proteins were extracted using Nuclei EZ Prep Nuclei Isolation kit (Sigma-Aldrich; Merck KGaA) according to the manufacturer's protocol. Western-blot analysis was used to detect the cytoplasmic and nuclear expression of various proteins.

**Dual-luciferase reporter assay.** 786-O cells were seeded in 6-well plates and transfected with Lipofectamine<sup>®</sup> 2000 (Invitrogen; Thermo Fisher Scientific, Inc.), along with TCF-responsive promoter reporter (TOP-flash) or nonresponsive control reporter (FOP-flash)  $\beta$ -catenin firefly luciferase reporter gene constructs (provided by Professor Mien-Chie Hung, University of Texas M. D. Anderson Cancer Center, Houston, USA), and a pRL-SV40 *Renilla* luciferase construct was used as the internal control for the reporter gene assay as previously described (12). Subsequently, cells were treated with silibinin and the luciferase activity was determined using a Dual-Luciferase Reporter Assay System (Promega Corporation). The ratio of TOP and FOP luciferase activity represented the transcriptional activity of  $\beta$ -catenin. Relative luciferase activity was represented as the mean  $\pm$  standard error of mean after normalizing to the control.

**Xenograft animal model.** A total of 10, 4-week-old BALB/c male nude mice (weight, 15-20 g) were purchased from the Laboratory Animal Center of Xi'an Jiaotong University. The nude mice were maintained in specific pathogen-free rooms that are carefully monitored for the presence of mouse pathogens. The rooms were kept at a temperature of 22-25°C, with a 12-h light/dark cycle and with free access to water and food. We operated the mice during the light phase in the daytime. The permission number for *in vivo* animal study is no. XJTULAC2019-1151. All animal care and experiments were approved by the Institutional Animal Care and Use Committee of Xi'an Jiaotong University. Animal health and behavior were monitored daily. Briefly, 786-O cells ( $2 \times 10^6$ ) were resuspended in 0.1 ml PBS and subcutaneously injected into the right flank of nude mice. When the tumor volume reached  $\sim 100$  mm<sup>3</sup>, the nude mice were randomly divided into two groups (n=5 mice per group): Control group and silibinin-treated group. The control group received treatment with the vehicle (oral gavage with saline) and the silibinin-treated group were fed by oral gavage with silibinin (150 mg/kg) every other day. The tumor sizes were measured every three days and the tumor volume was calculated as follows: Volume (mm<sup>3</sup>)=0.5 x (length) x (width)<sup>2</sup>. After 30 days, the mice were sacrificed using carbon dioxide (CO<sub>2</sub>) with a CO<sub>2</sub> displacement rate of 17.5% of chamber volume/min. the animals were exposed to CO<sub>2</sub> until complete cessation of breathing was observed for 10 min. Visually inspection of the animals for the absence of movement and respiration was performed. Death was assured by subsequent use of cervical dislocation. The tumors were weighed by electronic scales and prepared for immunohistochemical staining and western blot analysis.

For the metastatic model, 786-O cells were transfected with luciferase lentivirus and injected into the mice via the tail vein. The mice were randomly divided into the 2 aforementioned groups and treated as above. After 4 weeks, the mice were intraperitoneally injected with D-luciferin (150 mg/kg) and anesthetized with 10% chloral hydrate at a dose of 400 mg/kg by intraperitoneal injection. Then the mice were imaged using an IVIS Lumina II (PerkinElmer, Inc.) with Living Image software v4.5.4 (PerkinElmer, Inc.). The lung metastatic tumors were stained with hematoxylin for 10 min at room temperature and eosin for 1 min at room temperature.

**Statistical analysis.** All data are presented as the mean  $\pm$  standard deviation of at least three independent experiments. All statistical analyses were performed using GraphPad Prism 5.2 software (GraphPad Software, Inc.). The difference between various groups were analyzed using a one-way analysis of variance (ANOVA). Tukey's honestly significant difference post hoc test was used following one-way ANOVA. A Student's t-test was used for the comparisons between two groups. P<0.05 was considered to indicate a statistically significant difference.

## Results

**Silibinin inhibits migration and invasion in vitro.** In order to assess the inhibitory effects of silibinin on RCC cells, 786-O and ACHN cells were treated with different concentrations of silibinin for 24 h. The results indicated that a concentration

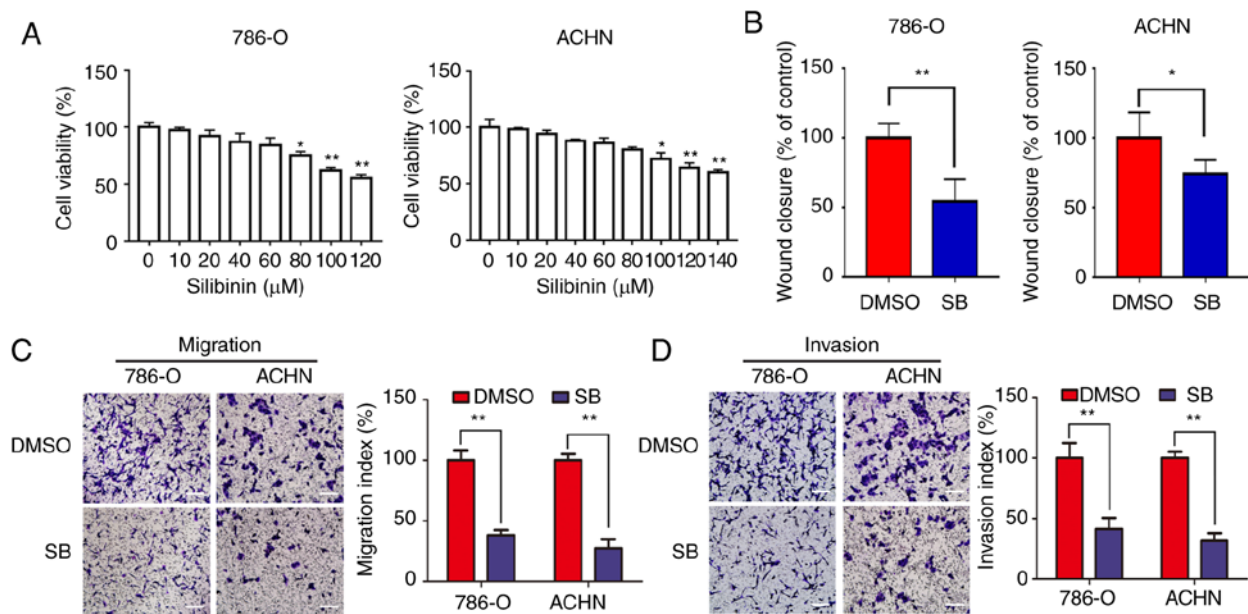


Figure 1. Inhibition of migration and invasion by SB in RCC cells. (A) RCC 786-O and ACHN cells were treated with different doses of SB for 24 h, and an MTT assay was used to measure cell viability. \* $P < 0.05$  and \*\* $P < 0.01$ . (B) Wound healing assays were performed on 786-O and ACHN cells treated with DMSO or 60  $\mu$ M SB. \* $P < 0.05$  and \*\* $P < 0.01$ . (C) Transwell migration and (D) invasion assays were used to detect the migratory and invasive properties of 786-O and ACHN cells treated with DMSO or 60  $\mu$ M SB for 24 h. Magnification,  $\times 100$ . Scale bar, 20  $\mu$ m. \*\* $P < 0.01$ . Results are shown as the mean  $\pm$  standard deviation of three experimental repeats. RCC, renal cell carcinoma; SB, silibinin.

$< 60 \mu$ M silibinin (SB) doesn't have significant effect on the proliferation of 786-O and concentration  $< 80 \mu$ M SB doesn't have significant effect on the proliferation of ACHN. As the concentration  $> 60 \mu$ M in 786-O and  $> 80 \mu$ M in ACHN can affect the cell viability, so 20/40/60  $\mu$ M SB was chosen in 786-O and 40/60/80  $\mu$ M SB in ACHN (Fig. 1A).

Migration of 786-O and ACHN cells was significantly inhibited by 60  $\mu$ M SB as determined by a wound healing assay (Fig. 1B). Similar results were obtained from the Transwell migration and invasion assays (Fig. 1C and D). Consistent with the authors' previous study (18), a low dose of SB ( $< 80 \mu$ M) significantly inhibited migration and invasion of RCC cells *in vitro*.

**SB suppresses EMT in RCC cells.** As described previously, EMT is one of the major mechanisms that regulates the metastatic progression of cancer (19). In RCC, EMT is known to be associated with migration and invasion (20). To evaluate whether the inhibitory effects of SB on migration and invasion was associated with EMT, the expression of EMT markers was measured using western blotting. As shown in Fig. 2A and B, SB increased the expression of E-cadherin and decreased the expression of the mesenchymal markers N-cadherin and vimentin in both a concentration- and time-dependent manner. To further demonstrate the effects of SB on EMT, cells were treated with TGF- $\beta$ 1, a well-known EMT inducer (21). TGF- $\beta$ 1-induced EMT, as determined by an increase in N-cadherin and vimentin expression and decrease in E-cadherin expression, and this was prevented by treatment with SB (Fig. 2C). The Transwell migration and invasion assays also showed that SB prevented TGF- $\beta$ 1-induced cell migration and invasion (Fig. 2D and E). Together, these results confirm that SB may inhibit RCC cell migration and invasion through preventing EMT.

**SB inhibits Wnt/ $\beta$ -catenin signaling in RCC cells.** Wnt/ $\beta$ -catenin signaling has been demonstrated to contribute to EMT and metastasis of RCC (22). Therefore, it was next determined if inhibition of EMT and metastasis by SB was associated with the Wnt/ $\beta$ -catenin signaling pathway. In the present study, together with upregulation of p- $\beta$ -catenin, downregulation of Wnt3a, p-GSK3 $\beta$  and  $\beta$ -catenin were also observed following treatment with SB (Fig. 3A). Decreased expression of total  $\beta$ -catenin was further confirmed by immunofluorescence analysis (Fig. 3B). In addition, a TOP-flash/FOP-flash luciferase reporter gene assay also showed that SB decreased the transcriptional activity of  $\beta$ -catenin (Fig. 3C). Consistent with this, SB decreased both the cytosolic and nuclear expression levels of  $\beta$ -catenin (Fig. 3D). Additionally, pretreatment with LiCl (a GSK3 $\beta$  kinase inhibitor) prevented the suppressive effects of SB on  $\beta$ -catenin (Fig. 3E).

**SB inhibits metastasis of RCC through downregulation of the Wnt/ $\beta$ -catenin signaling pathway.** To confirm the role of SB in regulating the Wnt/ $\beta$ -catenin signaling pathway,  $\beta$ -catenin was overexpressed in 786-O cells using plasmid transfections. As shown in Fig. 4A and B, overexpression of  $\beta$ -catenin reversed the effects of SB on EMT markers and metastatic activity. Although the inhibitory effects of SB on invasion showed no difference following knockdown of  $\beta$ -catenin using siRNA,  $\beta$ -catenin knockdown further enhanced the suppressive effects of SB on EMT markers and migration (Fig. 4C and D).

**SB inhibits EMT of RCC cells through autophagy-dependent Wnt/ $\beta$ -catenin signaling.** In the authors' previous study, it was demonstrated that autophagy induction by SB contributed to its reduction of metastasis in RCC cells (18); however, the underlying molecular mechanism was unknown. Consistent

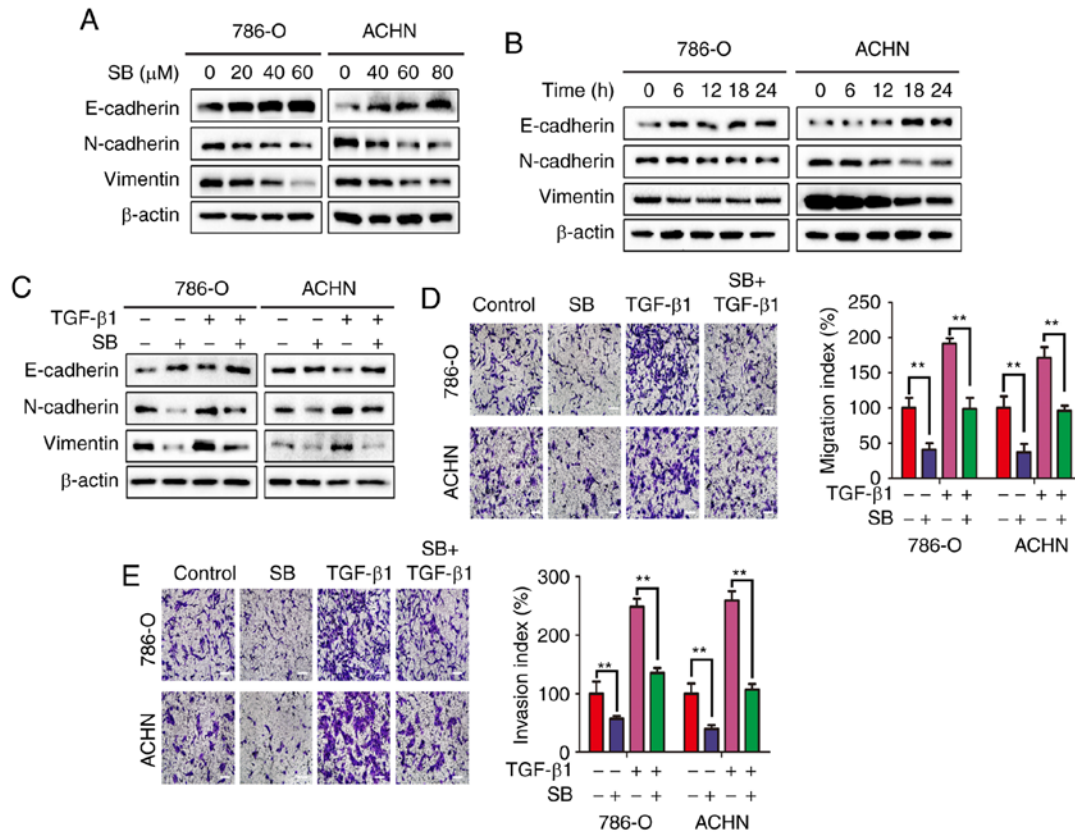


Figure 2. SB suppresses EMT in RCC cells. Expression of E-cadherin, N-cadherin and vimentin in 786-O and ACHN was detected by western blotting following treatment with different concentrations of SB for (A) 24 h or (B) 60  $\mu$ M SB for the indicated time intervals. (C) EMT markers were detected by western blot analysis following treatment with 60  $\mu$ M SB and 5 ng/ml TGF- $\beta$ 1 for 24 h.  $\beta$ -actin was used as the loading control. (D) Transwell migration and (E) invasion assays were performed in cells treated with 60  $\mu$ M SB and 5 ng/ml TGF- $\beta$ 1 for 24 h. DMSO treatment alone was used as the control. Magnification,  $\times 100$ . Scale bar, 20  $\mu$ m. \*\* $P < 0.01$ . Results are shown as the mean  $\pm$  standard deviation of three experimental repeats. RCC, renal cell carcinoma; EMT, epithelial-mesenchymal transition; SB, silibinin.

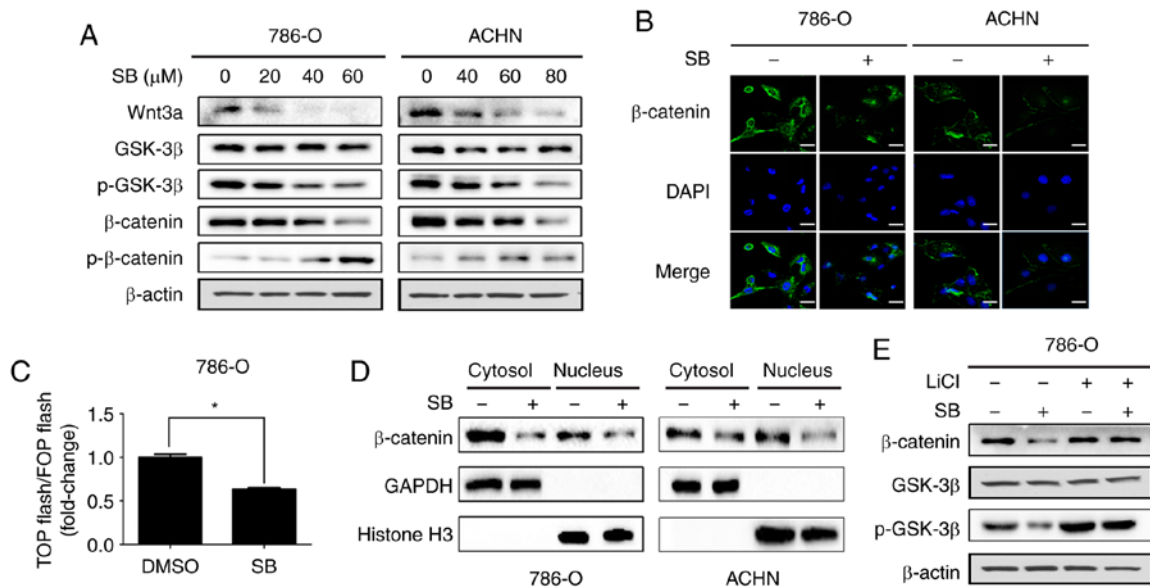


Figure 3. SB inhibits Wnt/ $\beta$ -catenin signaling in RCC cells. (A) Western blot analysis of Wnt/ $\beta$ -catenin signaling pathway associated protein expression levels in 786-O and ACHN cells treated with different doses of SB for 24 h.  $\beta$ -actin was used as the loading control. (B) Immunofluorescence analysis of  $\beta$ -catenin in 786-O and ACHN cells treated with 60  $\mu$ M of SB for 24 h. Scale bars, 20  $\mu$ m. (C) 786-O cells were transfected with TOP-flash or FOP-flash and treated with 60  $\mu$ M SB for 24 h before measuring luciferase activity by measuring the ratio between TOP and FOP. Relative luciferase activity is represented as the mean  $\pm$  standard deviation from each sample after normalizing to the control. \* $P < 0.05$ . (D) 786-O cells were treated with 60  $\mu$ M SB for 24 h. Western blotting was used to detect the cytosolic and nuclear expression levels of  $\beta$ -catenin. GAPDH and histone H3 were used as the cytosolic and nuclear controls, respectively. (E) 786-O cells were pre-treated with 20 mM LiCl for 6 h and subsequently treated with 60  $\mu$ M SB treatment for 24 h and western blot analysis was used to detect the protein expression levels of p-GSK3 $\beta$ , total GSK3 $\beta$  and  $\beta$ -catenin. TOP-flash, TCF-responsive promoter reporter; FOP-flash, nonresponsive control reporter; SB, silibinin; p-GSK, phosphorylated-glycogen synthase kinase.

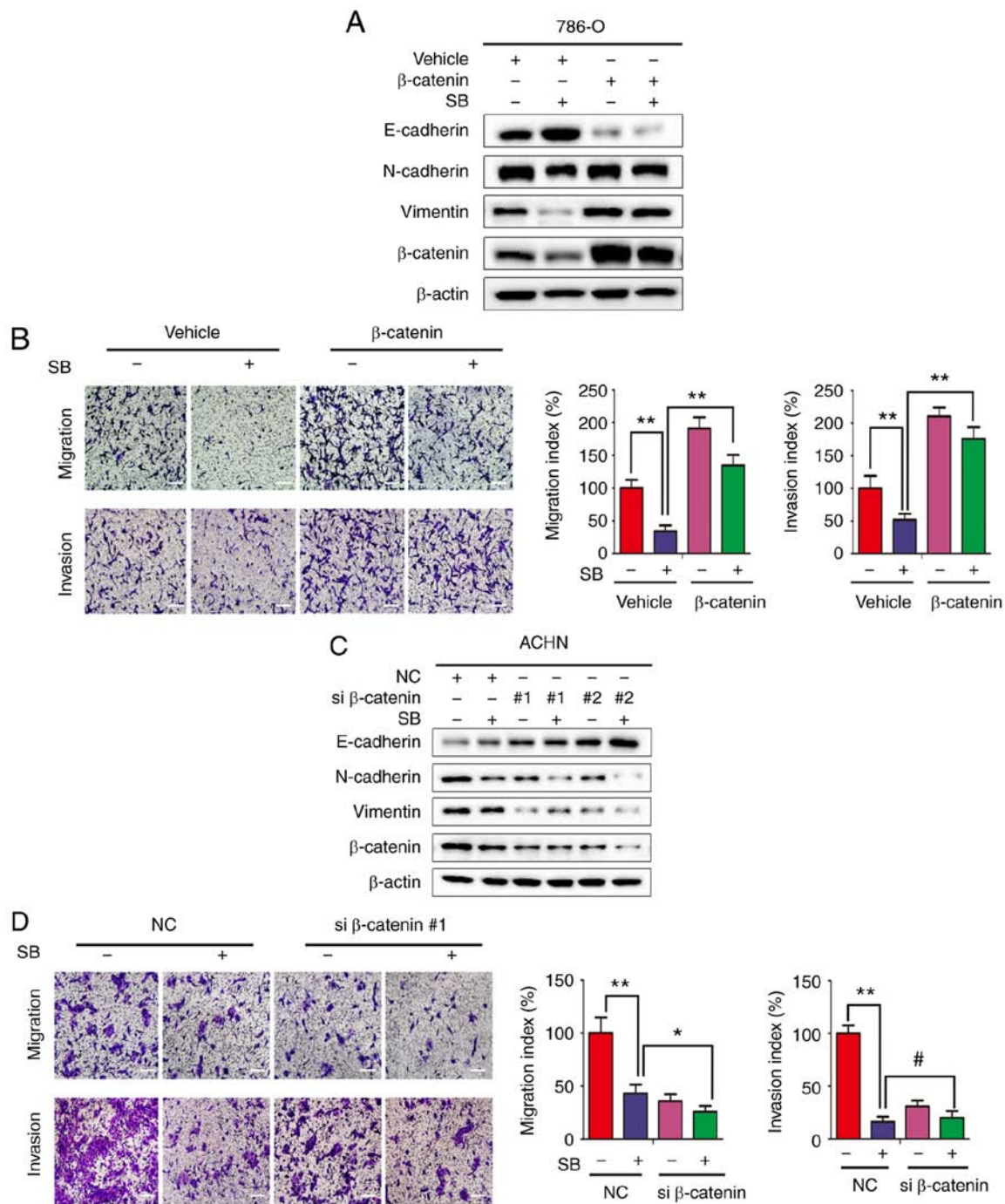
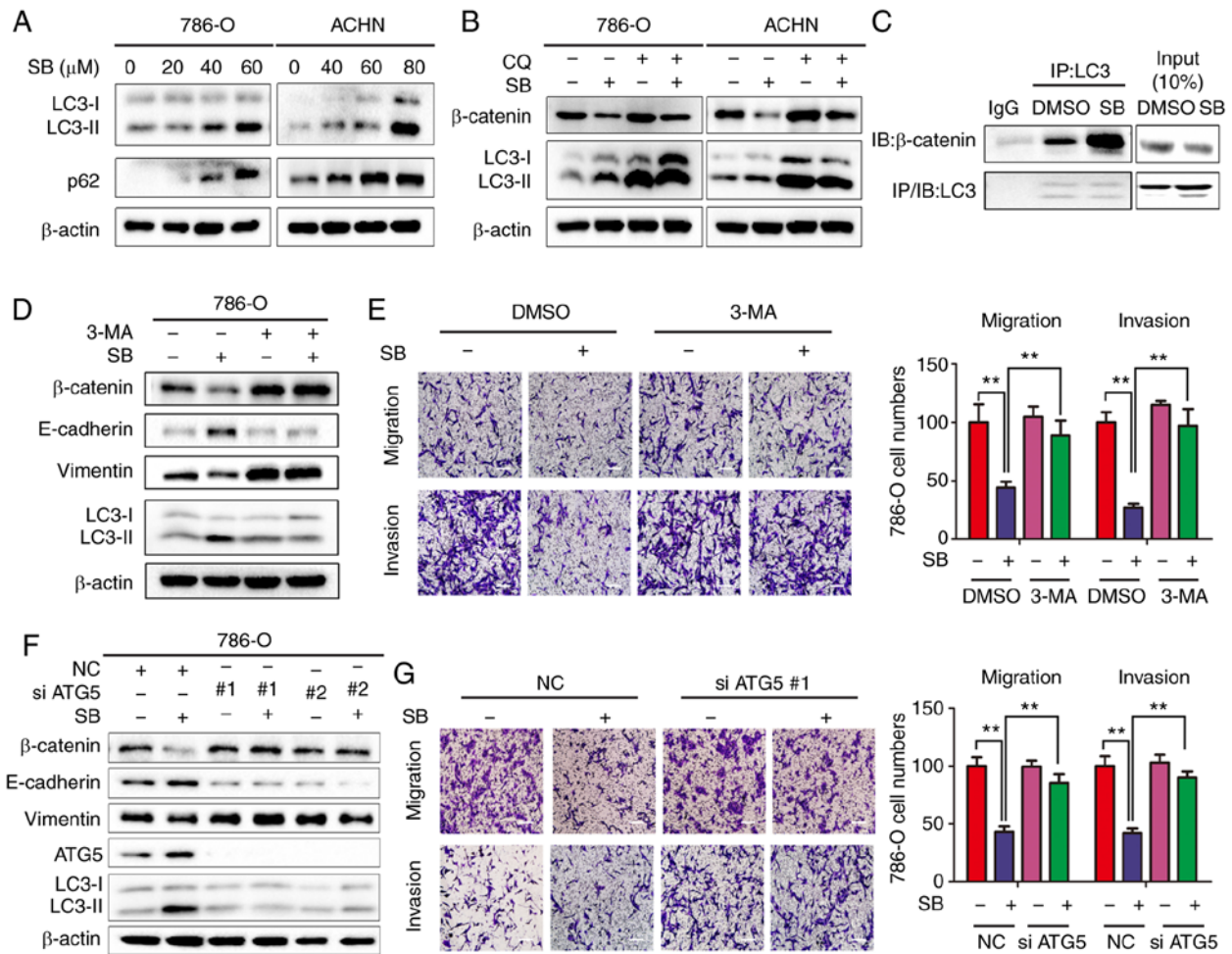


Figure 4. SB inhibits RCC metastasis through downregulating the Wnt/ $\beta$ -catenin pathway. (A)  $\beta$ -catenin-overexpressing 786-O cells were treated with 60  $\mu$ M SB for 24 h. Expression of EMT associated markers were determined by western blotting. (B) Transwell migration and invasion assays were performed in  $\beta$ -catenin-overexpressing 786-O cells following treatment with 60  $\mu$ M SB. Magnification, x100. Scale bar, 20  $\mu$ m. The experiment was repeated three times. \*\* $P$ <0.01. (C) ACHN cells were transfected with two different siRNA targeting  $\beta$ -catenin for 24 h and treated with DMSO or SB for another 24 h. Expression of EMT associated markers were determined by western blotting. (D) Transwell migration and invasion assays were performed on ACHN cells transfected with  $\beta$ -catenin siRNA sequence 1 following treatment with 60  $\mu$ M SB treatment. Magnification x100. Scale bar, 20  $\mu$ m. The experiment was repeated three times. # $P$ >0.05, \* $P$ <0.05 and \*\* $P$ <0.01. RCC, renal cell carcinoma; EMT, epithelial-mesenchymal transition; si, small interfering; SB, silibinin; N, neural; E, epithelial.

with the authors' previous findings (18), SB induced autophagy in RCC cells, as determined by the upregulation of LC3-II and p62 protein expression levels (Fig. 5A). As the interplay between Wnt/ $\beta$ -catenin signaling and autophagy has been identified previously (23,24), and  $\beta$ -catenin is known to be degraded through autophagy-lysosome system, the relationship between SB-induced autophagy and  $\beta$ -catenin downregulation was assessed. Inhibition of autophagy by

chloroquine (CQ), a lysosome inhibitor, resulted in increased expression of  $\beta$ -catenin in the presence of SB compared with SB treatment alone (Fig. 5B). Previous studies have shown that LC3 forms a complex with  $\beta$ -catenin, which promotes the lysosomal degradation of  $\beta$ -catenin (23,24). To further elucidate the underlying molecular mechanism, the effects of SB on the interaction between LC3 and  $\beta$ -catenin were determined using an immunoprecipitation assay. There was



**Figure 5.** SB induces inhibition of EMT via autophagy-dependent Wnt/ $\beta$ -catenin signaling in RCC cells. (A) Western blot analysis of LC3-I/II protein levels in 786-O and ACHN cells treated with different doses of SB.  $\beta$ -actin was used as the loading control. (B) 786-O and ACHN cells were treated with 60  $\mu$ M of SB for 24 h in the presence of 50  $\mu$ M CQ, and the protein expression levels of  $\beta$ -catenin and LC3-I/II were measured.  $\beta$ -actin was used as the loading control. (C) Co-immunoprecipitation of endogenous  $\beta$ -catenin and LC3 was assayed in 786-O cells following treatment with 60  $\mu$ M SB. (D) 786-O cells were pretreated with 3 mM 3-MA for 1 h, followed by treatment with 60  $\mu$ M of SB for 24 h. Western blot analysis was used to detect the expression levels of total  $\beta$ -catenin, E-cadherin, vimentin and LC3-I/II. (E) Transwell migration and invasion assays were performed on treated cells. Magnification,  $\times 100$ . Scale bar, 20  $\mu$ m. The experiment was repeated three times.  $^{**}P < 0.01$ . (F) 786-O cells were transfected with two siRNA sequences targeting ATG5 for 24 h and treated with DMSO or 60  $\mu$ M SB for another 24 h. Western blot analysis was used to detect the expression levels of total  $\beta$ -catenin, E-cadherin, vimentin, ATG5 and LC3-I/II.  $\beta$ -actin was used as the loading control. (G) Transwell migration and invasion assays were performed on treated cells under similar conditions. Magnification,  $\times 100$ . Scale bar, 20  $\mu$ m. The experiment was repeated three times.  $^{**}P < 0.01$ . EMT, epithelial-mesenchymal transition; CQ, chloroquine; IB, immunoblotting; IP, immunoprecipitation; ATG5, autophagy-associated gene 5; SB, silibinin; RCC, renal cell carcinoma; 3-MA, 3-methyladenine; NC, negative control; E, epithelial.

an increased level of interaction between LC3 and  $\beta$ -catenin following treatment with SB (Fig. 5C). Additionally, inhibition of initiation of autophagy by either 3-MA (Fig. 5D and E) or ATG5 knockdown (Fig. 5F and G) significantly attenuated the SB-induced suppression of cell migration and invasion, inhibition of EMT and downregulation of  $\beta$ -catenin, suggesting a vital role of autophagy-regulated  $\beta$ -catenin signaling in the anti-cancer effects of SB.

**SB inhibits RCC EMT and metastasis *in vivo*.** To verify the *in vitro* results, RCC subcutaneous and metastatic xenografts in nude mice were used as the *in vivo* model system. SB significantly decreased tumor growth and volume in RCC subcutaneous xenografts ( $P < 0.01$ ; Fig. 6A and B) without affecting the body weights of the nude mice (Fig. 6C). After 30 days, the average tumor weight of the control group was  $292.14 \pm 72.02$  mg, whereas in the SB-treated group it was

$163.68 \pm 43.23$  mg. Western blotting indicated that SB inhibited the expression of  $\beta$ -catenin and vimentin, whilst promoting the levels of E-cadherin and LC3-II (Fig. 6D). Downregulation of  $\beta$ -catenin and vimentin and upregulation of E-cadherin were further confirmed by immunohistochemistry (Fig. 6E).

Additionally, treatment with SB for 4 weeks inhibited lung metastasis induced by tail vein injection of 786-O cells *in vivo* (Fig. 6F). Collectively, these results were consistent with the *in vitro* results and suggested that SB inhibited RCC EMT and metastasis *in vivo* by regulating the autophagy-dependent Wnt/ $\beta$ -catenin signaling pathway.

## Discussion

SB is a traditional medicine extracted from milk thistle seeds and has been widely used in clinical practice as a hepatoprotective and antioxidative agent. Previous studies have

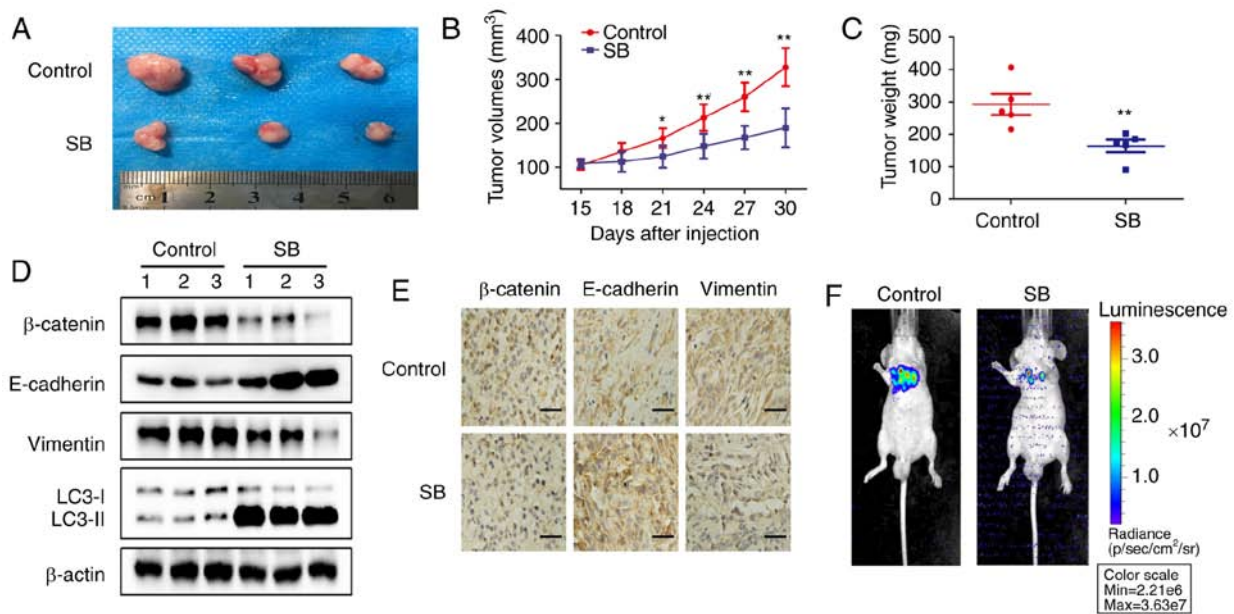


Figure 6. SB inhibits RCC EMT and metastasis *in vivo*. (A) 786-O cells were subcutaneously injected into male nude mice. Tumors were isolated from male BALB/c mice and measured. (B) Tumor volumes were measured every three days in the DMSO or SB treated mice. (C) After 30 days, the mice were sacrificed and tumor weights in mice injected with 786-O cells. Data are presented as the mean  $\pm$  standard deviation. \* $P < 0.05$  and \*\* $P < 0.01$ . (D) Western blot analysis of  $\beta$ -catenin, E-cadherin, vimentin and LC3-I/II expression in tumor xenografts. (E) Immunohistochemical analysis of  $\beta$ -catenin, E-cadherin and vimentin in tumor xenografts. (F) Luciferase-tagged 786-O cells were intravenously injected into male nude mice through the tail vein. Representative bioluminescence images of mice treated with DMSO or SB. ( $n = 5$ ). RCC, renal cell carcinoma; EMT, epithelial-mesenchymal transition; SB, silibinin; N, neural; E, epithelial.

demonstrated the anti-cancer properties of SB in various types of cancer, including breast cancer, gastric cancer, bladder cancer and prostate cancer (4-16). A previous study from the authors' laboratory has demonstrated the potential anti-cancer effects of SB against RCC (18), although the molecular mechanisms are yet to be identified. In the present study, a focus was placed on the interplay between  $\beta$ -catenin and autophagy. SB inhibited Wnt/ $\beta$ -catenin signaling *in vitro* and *in vivo* in an autophagy-dependent manner, which contributed to metastasis and EMT of 786-O and ACHN cells.

TGF- $\beta$ 1 treatment resulted in marginal change of both E-Cadherin and N-cadherin expression in 786-O cells, although enhanced invasion and migration ability of 786-O cells were observed. Complete EMT involves almost complete loss of epithelial markers and an increase in levels of several mesenchymal markers. Basically, the magnitude of change in the levels of the epithelial and mesenchymal markers can be used to distinguish between complete EMT and partial EMT (25). Therefore, a possible induction of partial EMT by TGF- $\beta$ 1 was proposed in the present study based on the changes of EMT markers. Partial EMT has received great attention by oncologists when compared with complete EMT (25,26). For partial EMT, cells simultaneously express epithelial and mesenchymal traits. Hence, they can initiate metastasis with incomplete loss of epithelial traits and/or incomplete gain of mesenchymal traits (27). Partial EMT in cancer cells is thought to enhance their invasive properties, generate circulating tumor cells and cancer stem cells, and promote resistance to anti-cancer drugs (26). Therefore, the ability of cancer cells to undergo partial EMT, rather than complete EMT, poses a higher metastatic risk. In the current study, enhanced invasive potential induced by TGF- $\beta$ 1 was observed in both 786-O and ACHN cells. Interestingly, this effect could be significantly

attenuated by SB treatment. Further studies focusing on the effects of SB on circulating tumor cells and cancer stem cells are needed to identify the exact role of SB on partial EMT in RCC induced by TGF- $\beta$ 1.

In the complex biological process of invasion and metastasis, tumor cells must adapt to different survival pressures. Autophagy, an intracellular physiological reaction, is regulated by numerous genes and their expression products. Autophagy can be activated to adapt to the metabolic stress and micro-environmental changes, and it is associated with EMT, inflammation, apoptosis and mechanisms of cancer metastasis (28,29). For cancer metastasis, autophagy serves varying roles at different stages. During the early stages, autophagy inhibits metastasis through maintaining genomic stability and reducing tumor inflammation; whereas, in the later stages of tumor progression, autophagy promotes metastasis by improving the survival ability of tumor cells (28). In the authors' previous study, SB decreased the metastatic capacity of RCC by activating autophagy through the AMPK/mTOR pathway (18). Autophagy induction by SB positively contributed to the anti-metastatic effects of SB against RCC. Although existing research has demonstrated the role of autophagy in promoting cell survival and therapeutic resistance (30-32), the relationship between autophagy and metastasis is obscure. In the present study, it was consistently demonstrated that SB decreased metastasis and EMT of RCC cells by inducing autophagy.

The Wnt/ $\beta$ -catenin signaling pathway participates in proliferation, invasion and metastasis of renal cancer cells, and effectively induces resistance and regeneration of renal cancer (33). Targeting the Wnt/ $\beta$ -catenin pathway inhibits the growth and metastasis of renal cancer and increases the sensitivity to chemotherapy. In bladder cancer, the authors'

laboratory previously demonstrated that SB inhibited  $\beta$ -catenin/ZEB1 signaling and decreased metastasis of bladder cancer (12). However, the effect of SB on  $\beta$ -catenin/ZEB1 signaling is still unclear. In the present study, it was demonstrated that SB-induced inactivation of Wnt/ $\beta$ -catenin signaling was associated with the inhibitory effects of SB on metastasis and EMT. Interestingly, in the present study, there was no statistical significance between the invasion results of SB and SB+siRNA  $\beta$ -catenin groups. The reasons that contributed to this phenomenon are still unclear. One possible mechanism is that different signaling pathways may play different roles in mediating cancer cell migration and invasion. Further study is needed to explore the possible mechanisms.  $\beta$ -catenin negatively regulates the formation of the autophagosome and has direct inhibitory effects on the expression of p62 via TCF4 (23). Furthermore, LC3 or p62 directly interacts with  $\beta$ -catenin for lysosomal-autophagic degradation (23,24). In the present study, increased lysosomal degradation of  $\beta$ -catenin and enhanced interactions between LC3 and  $\beta$ -catenin were observed following SB treatment in RCC cells.

In summary, the present study identified a novel mechanism by which SB regulated metastasis and EMT of RCC *in vitro* and *in vivo*, in which activation of autophagy by SB treatment resulted in degradation of  $\beta$ -catenin. The data highlight the clinical potential of SB for treating patients with RCC and further demonstrates that increasing  $\beta$ -catenin degradation in autophagy-lysosome pathway may be a promising target for treating RCC.

#### Acknowledgements

The authors would like to thank Professor Mien-Chie Hung (China Medical University, Taichung, Taiwan, China) for supplying the TOP-flash and FOP-flash  $\beta$ -catenin firefly luciferase reporter gene constructs.

#### Funding

The present study was funded by National Natural Science Foundation of China (grant nos. 81101936 and 81672538).

#### Availability of data and materials

All data generated or analyzed during this study are included in this published article.

#### Authors' contributions

YF, TH, LL and JZ conceived and designed experiments. YF, TH, WD, TL, JL and BL performed all experiments. YF, TH, LL and JZ analyzed the data. YF, LL and JZ wrote and revised the manuscript. All authors read and approved the final manuscript.

#### Ethics approval and consent to participate

All animal care and experiments were approved by the Institutional Animal Care and Use Committee of Xi'an Jiaotong University. The permission number for *in vivo* animal study is no. XJTULAC2019-1151.

#### Patient consent for publication

Not applicable.

#### Competing interests

The authors declare that they have no competing interests.

#### References

- Ljungberg B, Bensalah K, Canfield S, Dabestani S, Hofmann F, Hora M, Kuczyk MA, Lam T, Marconi L, Merseburger AS, *et al*: EAU guidelines on renal cell carcinoma: 2014 update. *Eur Urol* 67: 913-924, 2015.
- Capitanio U, Bensalah K, Bex A, Boorjian SA, Bray F, Coleman J, Gore JL, Sun M, Wood C and Russo P: Epidemiology of renal cell carcinoma. *Eur Urol* 75: 74-84, 2019.
- Singer EA, Gupta GN and Srinivasan R: Update on targeted therapies for clear cell renal cell carcinoma. *Curr Opin Oncol* 23: 283-289, 2011.
- Cheung CW, Gibbons N, Johnson DW and Nicol DL: Silibinin-a promising new treatment for cancer. *Anticancer Agents Med Chem* 10: 186-195, 2010.
- Zeng J, Liu W, Fan YZ, He DL and Li L: PrLZ increases prostate cancer docetaxel resistance by inhibiting LKB1/AMPK-mediated autophagy. *Theranostics* 8: 109-123, 2018.
- Li F, Sun Y, Jia J, Yang C, Tang X, Jin B, Wang K, Guo P, Ma Z, Chen Y, *et al*: Silibinin attenuates TGF  $\beta$ 1 induced migration and invasion via EMT suppression and is associated with COX2 downregulation in bladder transitional cell carcinoma. *Oncol Rep* 40: 3543-3550, 2018.
- Dheeraj A, Rigby CM, O'Bryant CL, Agarwal C, Singh RP, Deep G and Agarwal R: Silibinin treatment inhibits the growth of Hedgehog inhibitor-resistant basal cell carcinoma cells via targeting EGFR-MAPK-Akt and Hedgehog signaling. *Photochem Photobiol* 93: 999-1007, 2017.
- Rigby CM, Roy S, Deep G, Guillermo-Lagae R, Jain AK, Dhar D, Orlicky DJ, Agarwal C and Agarwal R: Role of p53 in silibinin-mediated inhibition of ultraviolet B radiation-induced DNA damage, inflammation and skin carcinogenesis. *Carcinogenesis* 38: 40-50, 2017.
- Deep G, Kumar R, Nambiar DK, Jain AK, Ramteke AM, Serkova NJ, Agarwal C and Agarwal R: Silibinin inhibits hypoxia-induced HIF-1 $\alpha$ -mediated signaling, angiogenesis and lipogenesis in prostate cancer cells: *In vitro* evidence and *in vivo* functional imaging and metabolomics. *Mol Carcinog* 56: 833-848, 2017.
- Ting H, Deep G, Kumar S, Jain AK, Agarwal C and Agarwal R: Beneficial effects of the naturally occurring flavonoid silibinin on the prostate cancer microenvironment: Role of monocyte chemoattractant protein-1 and immune cell recruitment. *Carcinogenesis* 37: 589-599, 2016.
- Bosch-Barrera J and Menendez JA: Silibinin and STAT3: A natural way of targeting transcription factors for cancer therapy. *Cancer Treat Rev* 41: 540-546, 2015.
- Wu K, Ning Z, Zeng J, Fan J, Zhou J, Zhang T, Zhang L, Chen Y, Gao Y, Wang B, *et al*: Silibinin inhibits beta-catenin/ZEB1 signaling and suppresses bladder cancer metastasis via dual-blocking epithelial-mesenchymal transition and stemness. *Cell Signal* 25: 2625-2633, 2013.
- Raina K, Agarwal C, Wadhwa R, Serkova NJ and Agarwal R: Energy deprivation by silibinin in colorectal cancer cells: A double-edged sword targeting both apoptotic and autophagic machineries. *Autophagy* 9: 697-713, 2013.
- Zeng J, Sun Y, Wu K, Li L, Zhang G, Yang Z, Wang Z, Zhang D, Xue Y, Chen Y, *et al*: Chemopreventive and chemotherapeutic effects of intravesical silibinin against bladder cancer by acting on mitochondria. *Mol Cancer Ther* 10: 104-116, 2011.
- Li L, Zeng J, Gao Y and He D: Targeting silibinin in the antiproliferative pathway. *Expert Opin Investig Drugs* 19: 243-255, 2010.
- Cui W, Gu F and Hu KQ: Effects and mechanisms of silibinin on human hepatocellular carcinoma xenografts in nude mice. *World J Gastroenterol* 15: 1943-1950, 2019.
- Liang L, Li L, Gao Y, Chen YL, Wang ZQ, Wang XY, Chang LS and He D: Inhibitory effect of silibinin on EGFR signal-induced renal cell carcinoma progression via suppression of the EGFR/MMP-9 signaling pathway. *Oncol Rep* 28: 999-1005, 2012.

18. Li F, Ma Z, Guan Z, Chen Y, Wu K, Guo P, Wang X, He D and Zeng J: Autophagy induction by silibinin positively contributes to its anti-metastatic capacity via AMPK/mTOR pathway in renal cell carcinoma. *Int J Mol Sci* 16: 8415-8429, 2015.
19. Smith BN and Bhowmick NA: Role of EMT in metastasis and therapy resistance. *J Clin Med* 5: E17, 2016.
20. Piva F, Giulietti M, Santoni M, Occhipinti G, Scarpelli M, Lopez-Beltran A, Cheng L, Principato G and Montironi R: Epithelial to mesenchymal transition in renal cell carcinoma: Implications for cancer therapy. *Mol Diagn Ther* 20: 111-117, 2016.
21. Tsuda T: Extracellular interactions between fibulins and transforming growth factor (TGF)- $\beta$  in physiological and pathological conditions. *Int J Mol Sci* 19: 2787, 2018.
22. Xu Q, Krause M, Samoylenko A and Vainio S: Wnt signaling in renal cell carcinoma. *Cancers (Basel)* 8: 57, 2016.
23. Petherick KJ, Williams AC, Lane JD, Ordonez-Moran P, Huelsken J, Collard TJ, Smartt HJ, Batson J, Malik K, Paraskeva C and Greenhough A: Autolysosomal  $\beta$ -catenin degradation regulates Wnt-autophagy-p62 crosstalk. *Embo J* 32: 1903-1916, 2013.
24. Jia Z, Wang J, Wang W, Tian Y, XiangWei W, Chen P, Ma K and Zhou C: Autophagy eliminates cytoplasmic beta-catenin and NICD to promote the cardiac differentiation of P19CL6 cells. *Cell Signal* 26: 2299-2305, 2014.
25. Grigore AD, Jolly MK, Jia D, Farach-Carson MC and Levine H: Tumor Budding: The Name is EMT. Partial EMT. *J Clin Med* 5: 51, 2016.
26. Saitoh M: Involvement of partial EMT in cancer progression. *J Biochem* 164: 257-264, 2018.
27. Christiansen JJ and Rajasekaran AK: Reassessing epithelial to mesenchymal transition as a prerequisite for carcinoma invasion and metastasis. *Cancer Res* 66: 8319-8326, 2006.
28. Mowers EE, Sharifi MN and Macleod KF: Autophagy in cancer metastasis. *Oncogene* 36: 1619-1630, 2017.
29. Levy J, Towers CG and Thorburn A: Targeting autophagy in cancer. *Nat Rev Cancer* 17: 528-542, 2017.
30. Li YJ, Lei YH, Yao N, Wang CR, Hu N, Ye WC, Zhang DM and Chen ZS: Autophagy and multidrug resistance in cancer. *Chin J Cancer* 36: 52, 2017.
31. Smith AG and Macleod KF: Autophagy, cancer stem cells and drug resistance. *J Pathol* 247: 708-718, 2019.
32. Das CK, Mandal M and Kögel D: Pro-survival autophagy and cancer cell resistance to therapy. *Cancer Metastasis Rev* 37: 749-766, 2018.
33. Guillen-Ahlers H: Wnt signaling in renal cancer. *Curr Drug Targets* 9: 591-600, 2008.



This work is licensed under a Creative Commons Attribution-NonCommercial-NoDerivatives 4.0 International (CC BY-NC-ND 4.0) License.